JPE 18-4-14

https://doi.org/10.6113/JPE.2018.18.4.1099
ISSN(Print): 1598-2092 / ISSN(Online): 2093-4718

Loss Minimization Control of Interior Permanent Magnet Synchronous Motors Considering Self-Saturation and Cross-Saturation

Hamidreza Pairo†, Mohammad Khanzade**, and Abbas Shoulaie*

†,*Dept. of Electrical Engineering, Iran University of Science and Technology, Tehran, Iran
**Dept. of Information and Communication Technology, Comprehensive Imam Hosein University, Tehran, Iran

Abstract

In this paper, a loss minimization control method for interior permanent magnet synchronous motors is presented with considering self-saturation and cross saturation. According to variation of the d-axis and q-axis inductances by different values of the d-axis and q-axis components of currents, it is necessary to consider self-saturation and cross saturation in the loss minimization control method. In addition, the iron loss resistance variation due to frequency variation is considered in the condition of loss minimization. Furthermore, the loss minimization control method is compared with maximum torque per ampere (MTPA), unity power factor (UPF) and i_d=0 control methods. Experimental results verify the performance and proper dynamic response of the loss minimization control method with considering self-saturation and cross saturation.

Key words: Loss minimization, Maximum efficiency control method, Permanent magnet synchronous motor, Self-saturation and cross-saturation

I. INTRODUCTION

Due in large part to energy prices and energy efficiency policies, energy saving has become very important. However, electrical motors consume a great deal of power. Therefore, reducing the loss of electrical motors by just a few percent has a great impact on total power consumption. Permanent magnet synchronous motors have some advantages including high efficiency, high energy-density, fast dynamic response, etc. As a result of these advantages, PMSMs have been widely used in industrial drive applications, mainly for efficiency improvement [1]-[6].

There are a number of methods to control permanent magnet synchronous motors such as the i_d=0 control method [7], 'unity power factor' [8], [9] 'maximum torque per ampere' [10]-[12], loss-minimization, etc. Among these methods, the loss- minimization control methods are highly appreciated in comparison with others for their energy-savings.

The I_d=0 control method is the most conventional control method for permanent magnet synchronous motors. This method, by linearization of the relation between the torque and the current, results in simplifying the control method. In the 'maximum torque per ampere' control method, the d-axis stator current is adjusted in such a way that minimizes the copper loss and maximizes the ratio of the torque to stator current. In the 'unity power factor' control method, the d-axis current is derived in such a way that the angle between the current and the voltage becomes zero. Although reactive power is zero in this method, the loss is not minimized. Therefore, the efficiency decreases to some extent.

Loss-minimization techniques can be divided into two main approaches including model-based and search-based control methods. Generally, these methods are applicable to induction motors [13]-[16] and permanent magnet synchronous motors [17]-[21].

In the search-based methods, the control variables (including the d-axis current, V/f ratio, etc) are perturbed and then the direction of the input power variation is observed to determine the direction of changing the control variable. In [19], the filtered dc-link current is used as an input signal to determine

Manuscript received Jul. 13, 2017; accepted Apr. 11, 2018
Recommended for publication by Associate Editor Zheng Wang.
†Corresponding Author: h_pairo@elec.iust.ac.ir
Tel: +982177945316, Iran University of Science and Technology
*Dept. of Electrical Eng., Iran Univ. of Science and Tech., Iran
**Dept. of Inform. and Commun. Tech., Comprehensive Imam Hosein University, Iran

the direction of the input power variation, which specifies the V/f ratio for the next iteration. Generally, the major advantages of search-based methods are parameter independence and simplicity in implementation. The main drawbacks are an oscillation around the optimum operating point and a low dynamic response. These drawbacks limit the utilization of search-based methods in some applications where model-based methods should be utilized. In addition, search-based methods have slow response times and unexpected torque disturbances. In each iteration, after implementing a new step of i_d, it should wait to reach steady-state. Then next step is implemented.

Model-based methods depend on motor parameters. The loss model of permanent magnet synchronous motors is utilized in model-based loss minimization control methods. The losses of a motor can be divided into two types. These two types are controllable loss and non-controllable loss. The controllable loss includes copper loss and iron loss. These losses can be controlled via changing the motor flux by controlling the d-axis current. Therefore, in model-based methods, the motor loss equation is differentiated with respect to the d-axis current and the resulting expression is equated to zero to achieve the loss minimization condition [21]. Based on [20], for SPM motors (L_d=L_q), the loss-minimization condition is easily implementable. However, the loss-minimization condition for salient pole PMSMs is more complicated and cannot be easily achieved due to the nonlinear relationship nature of the equations. Therefore, the optimum value of i_d is approximated with a degree 2 polynomial expression as a function of i_q. In this expression, coefficients are a function of the speed. The main drawbacks are calculating a lot of coefficients for using in a look-up table and that fact that these calculations should be repeated again for a new motor [18]. Accordingly, in [21], the optimum i_d is obtained as a function of the speed and i_q. This equation is fairly straightforward. However, the loss-model requires some parameters which can be obtained via extra tests under different speeds and different loads.

In this paper, loss model of permanent magnet synchronous motors is investigated in Section II. In Section. III, the condition of the maximum torque per ampere and the unity power factor control methods are discussed. In Section IV, the condition of loss minimization is obtained with considering self-saturation and cross saturation. In Section. V, the motor parameters including the self-saturation, cross saturation and iron loss resistance variation due to the frequency are discussed. In section V, the performance of the proposed method is evaluated by experimental results. Some conclusions are presented in Section VII.

II. Loss Model of Permanent Magnet Synchronous Motors

A steady-state equivalent circuit of a permanent magnet synchronous motor considering the iron loss is shown in Fig. 1.

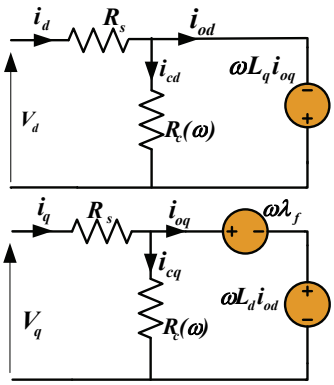

Fig. 1. Steady-state equivalent circuit of a PMSM.

From the equivalent circuit in Fig. 1, the copper and iron losses are expressed as:

$$P_{cu} = R_s(i_d^2 + i_q^2) \tag{1}$$

$$P_{Fe} = R_c(i_{cd}^2 + i_{cq}^2)$$

Where:

$$i_d = i_{od} + i_{cd}; \qquad i_{cd} = -\frac{\omega L_q}{R_c} i_{oq} \tag{2}$$

$$i_q = i_{oq} + i_{cq}; \qquad i_{cq} = \frac{\omega(L_d i_{od} + \lambda_f)}{R_c} \tag{3}$$

$$V_d = R_s i_d - \omega L_q i_{oq} \tag{4}$$

$$V_q = R_s i_q + \omega(L_d i_{od} + \lambda_f) \tag{5}$$

In addition, the torque equation is as follows:

$$T = P i_{oq}\left(\lambda_f + (L_d - L_q) i_{od}\right) \tag{6}$$

Inductance: In the loss-minimization method, i_d and i_q vary under different loads and speeds. Therefore, the self-saturation and cross-saturation effects should be considered. For considering self-saturation and cross-saturation effects on L_d and L_q, linear approximations are utilized for L_d and L_q for use in the loss-minimization method:

$$L_q = L_{q0}\left(1 - \frac{\alpha_1}{L_{q0}} i_{oq} - \frac{\beta_1}{L_{q0}} i_{od}\right) \tag{7}$$

$$L_d = L_{d0}\left(1 - \frac{\alpha_2}{L_{d0}} i_{oq} - \frac{\beta_2}{L_{d0}} i_{od}\right)$$

L_{d0} and L_{q0} are constant terms of (7). In addition, α_1, β_1, α_2 and β_2 are coefficients of the d-axis and q-axis currents in the equation for linear approximation of the d-axis and q-axis inductances. In this equation, the coefficients are obtained by performing curve fitting on the measured values of the d-axis and q-axis inductances via curve fitting toolbox (cftool) in MATLAB.

Iron loss resistance ($R_c(\omega)$): $R_c(\omega)$ varies under variable speed operation due to frequency dependency. Therefore, for the loss-minimization method, it is needed to identify the iron loss resistance as a function of speed.

III. Conditions of Different Control Methods

In the 'unity power factor' control method, the d-axis current is derived in such a way that the angle between the current and the voltage becomes zero. By equating the power factor angle (φ) to zero in the equation of tan (δ+φ) = V_q/V_d , the condition of the 'unity power factor' control method can be obtained as follows [4]:

$$i_d = \frac{-\lambda_f + \sqrt{\lambda_f^2 - 4L_d L_q i_q^2}}{2L_d} \tag{8}$$

In the MTPA control method, the torque per ampere ratio should be calculated. Then the result should be differentiated with respect to the d-axis current and equating the derivative to zero. Therefore, the result is the condition of the MTPA control method [12]:

$$i_d = \frac{-\lambda_f - \sqrt{\lambda_f^2 + 4(L_d - L_q)^2 i_q^2}}{2(L_d - L_q)} \tag{9}$$

IV. Loss-Minimization Method Considering Self-Saturation and Cross Saturation

In the loss-minimization control method, the d-axis current is controlled in such a way that the total controllable loss (the sum of the copper and iron losses) is minimized. First, the copper and iron losses should be calculated using (1), (2) and (3). The differentiation of i_{oq}, the copper loss and the iron loss with respect to i_{od} are as follow:

$$\frac{di_{oq}}{di_{od}} = \frac{(\beta_2 - \beta_1) i_{od} i_{oq} - (L_d - L_q) i_{oq}}{(\lambda_f + (L_d - L_q) i_{od} - (\alpha_2 - \alpha_1) i_{od} i_{oq})} \tag{10}$$

$$\frac{dP_{cu}}{di_{od}} = 2R_s \left\{ \left(i_{od} - \frac{\omega L_q}{R_c} i_{oq} \right) \left(\left(1 + \frac{\omega \beta_1}{R_c} i_{oq} \right) + \right. \right. \tag{11}$$

$$\left(\frac{\omega(\alpha_1 i_{oq} - L_q)}{R_c} \right) \cdot \frac{(\beta_2 - \beta_1) i_{od} i_{oq} - (L_d - L_q) i_{oq}}{(\lambda_f + (L_d - L_q) i_{od} - (\alpha_2 - \alpha_1) i_{od} i_{oq})} \Bigg)$$

$$+ \left(i_{oq} + \frac{\omega(L_d i_{od} + \lambda_f)}{R_c} \right) \cdot \left(\left(1 - \frac{\omega \alpha_2 i_{od}}{R_c} \right) \cdot \right.$$

$$\left. \left. \frac{(\beta_2 - \beta_1) i_{od} i_{oq} - (L_d - L_q) i_{oq}}{(\lambda_f + (L_d - L_q) i_{od} - (\alpha_2 - \alpha_1) i_{od} i_{oq})} + \frac{\omega(L_d - \beta_2 i_{od})}{R_c} \right) \right\}$$

$$\frac{dP_{Fe}}{di_{od}} = \frac{2\omega^2 L_q i_{oq}}{R_c}. \tag{12}$$

$$\left((L_q - \alpha_1 i_{oq}) \cdot \frac{(\beta_2 - \beta_1) i_{od} i_{oq} - (L_d - L_q) i_{oq}}{(\lambda_f + (L_d - L_q) i_{od} - (\alpha_2 - \alpha_1) i_{od} i_{oq})} \right.$$

$$\left. - \beta_1 i_{oq} \right) + \frac{2\omega^2 (L_d i_{od} + \lambda_f)}{R_c}.$$

$$\left((-\alpha_2 i_{od}) \cdot \frac{(\beta_2 - \beta_1) i_{od} i_{oq} - (L_d - L_q) i_{oq}}{(\lambda_f + (L_d - L_q) i_{od} - (\alpha_2 - \alpha_1) i_{od} i_{oq})} \right.$$

$$\left. + L_d - \beta_2 i_{od} \right)$$

It should be noted that α_1, α_2, β_1 and β_2 are linear approximation coefficients of L_d and L_q (due to self-saturation and cross-saturation). Therefore, the loss-minimization condition is achieved by differentiating the sum of the copper and iron losses with respect to i_{od}, and equating the result to zero:

$$\frac{dP_{Fe}}{di_{od}} + \frac{dP_{cu}}{di_{od}} = 0 \rightarrow \tag{13}$$

$$\left\{ -\omega^2 (R_s + R_c) L_d \left((L_d - L_q) \beta_2 - \right. \right.$$

$$\left. \left. (\alpha_2 \beta_1 - \alpha_1 \beta_2) i_{oq} \right) \right\} i_{od}^3$$

$$+ \left\{ (L_d - L_q - (\alpha_2 - \alpha_1) i_{oq}) \left(R_s R_c^2 + \omega^2 (R_s + R_c) \right. \right.$$

$$\left. \left(L_d^2 - \beta_2 \lambda_f \right) \right) - \omega^2 (R_s + R_c) \left(\beta_2 \lambda_f L_d + \right.$$

$$\left. \left. (\beta_2 - \beta_1) \alpha_2 \lambda_f i_{oq} - (L_d - L_q) \alpha_2 L_d i_{oq} \right) \right\} i_{od}^2$$

$$+ \left\{ R_s R_c^2 \left(\lambda_f + (\beta_2 - \beta_1) i_{oq}^2 \right) + \omega^2 (R_s + R_c) \cdot \right.$$

$$\left(2\lambda_f L_d^2 - L_d L_q \lambda_f + \alpha_1 L_d \lambda_f i_{oq} - L_q \beta_1 i_{oq}^2 + \right.$$

$$\alpha_2 \beta_1 L_q i_{oq}^3 - \alpha_2 L_q \lambda_f i_{oq} + \beta_2 \left(L_q^2 i_{oq}^2 - \alpha_1 L_q i_{oq} \right.$$

$$\left. \left. \left. - \lambda_f^2 \right) \right) \right\} i_{od}$$

$$+ \left\{ -R_s R_c^2 (L_d - L_q) i_{oq}^2 + \omega^2 (R_s + R_c) \cdot \left((L_d - L_q) \right. \right.$$

$$\left. \left. \left(\alpha_1 L_q i_{oq}^3 - L_q^2 i_{oq}^2 \right) + \lambda_f^2 L_d - \lambda_f L_q \beta_1 i_{oq}^2 \right) \right\} = 0$$

Equation (13) is as a function of i_{od}, i_{oq} and ω. It should be noted that R_c varies with speed. In addition, L_d and L_q vary with the current.

For implementing the condition of loss-minimization (13), a PI-controller is used to achieve this condition Therefore, equation (13) is calculated. It should be noted that the calculations are performed in every specified fixed time steps. For performing the calculations in each step, the output value of the PI-controller from the previous step ($i_d^{*(n-1)}$) is utilized in the calculation of equation (13). The result of calculating equation (13) is applied to the PI-controller. The

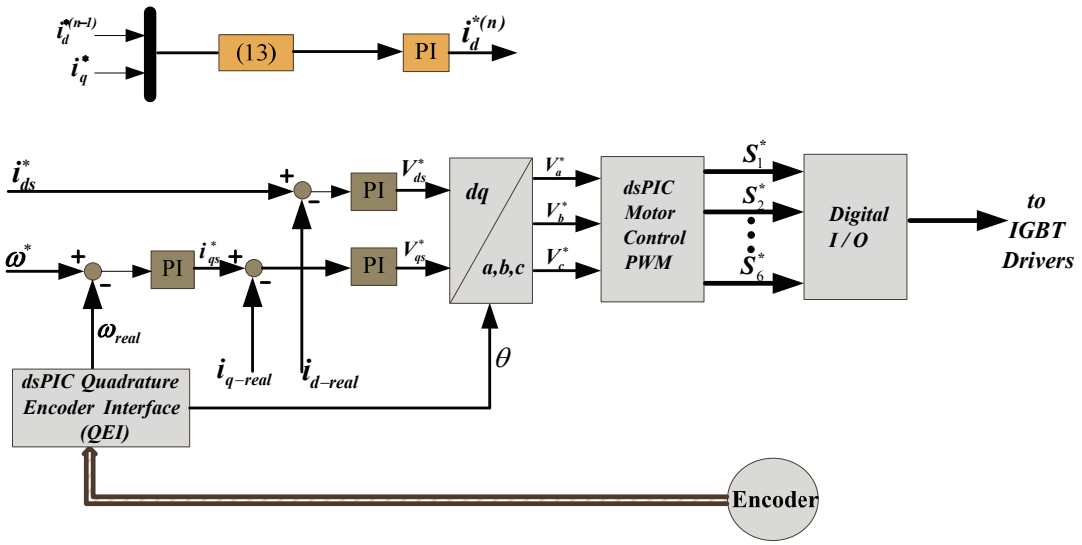

Fig. 2. Block diagram of the control system.

output value of the PI-controller is utilized as the reference value of the d-axis current for the current step ($i_d^{*(n)}$). Based on this procedure, the PI-controller adjusts the d-axis current in such a way that the output value of the block for the calculation of (13) (or the input value of the PI-controller) becomes zero. Therefore, by the zero value of the calculation result of (13), the condition of the loss-minimization is satisfied and the efficiency is maximized.

The q-axis current is utilized as the output of the speed controller. In addition, the q-axis current is directly used in the block for calculating the condition of the optimum value of the d-axis current (13), which leads to a simplification of the implementation. On the other hand, the relations between i_d, i_q, i_{oq} and i_{od} are expressed in equations (2)-(3). By determining i_d and i_q (in the control system), i_{oq} and i_{od} can be achieved for utilization in equation (13) based on (2)-(3).

V. Permanent Magnet Synchronous Motor Parameters

Motor parameters are shown in Table I. The measured q-axis and d-axis inductances in different i_{od} and i_{oq} are shown in Fig. 3(a) and Fig. 3(b), respectively. The d-axis and q-axis inductances are approximated by a linear function of i_{od} and i_{oq} (in order to consider the self-saturation and cross-saturation in the loss-minimization method). The linear approximation coefficients of (7) are shown in Table I. The coefficients of L_{q0}, L_{d0}, α_1, β_1, α_2 and β_2 are obtained via a curve-fitting on the measured values of d-axis and q-axis inductances.

The iron loss resistance is measured based on an offline method presented in [22]. Based on the procedure for measuring the iron loss resistance and stray loss components of the torque (T_f), the motor operates under a constant speed and no-load condition. Afterwards, by changing i_d, the semi-input power (the input power minus the copper loss) and the square of speed emf are calculated for each specified speed [22]:

$$P_{si} = P_{in} - R_s\left(i_d^2 + i_q^2\right) = P_{in} - 3R_s i_{rms}^2 \tag{14}$$

$$\omega_s^2\left(\lambda_d^2 + \lambda_q^2\right) = \left(V_q - R_s i_q\right)^2 + \left(V_d - R_s i_d\right)^2$$

Therefore, the inverse of the slope of the linear function is the iron loss resistance. In addition, the intersection of the linear function with the vertical axis (in the no-load condition) is the sum of the mechanical and stray losses at a specified

TABLE I
Motor Parameters

$R_s(\Omega)$	0.131
$R_c(\Omega)$	Fig. 5-b
L_d(H)	Fig. 3-b
L_q(H)	Fig. 3-a
L_{q0}	0.004027
α_1	4.374×10^{-5}
β_1	5.838×10^{-6}
L_{d0}	0.001922
α_2	1.154×10^{-6}
β_2	3.078×10^{-6}
λ_f(wb)	0.109
J(Kg.m^2)	0.0041
Friction and Windage Torque(N.m)	0.391(@2000rpm)
Number of Pole Pairs	4
Rated Speed(rpm)	2000
Rated Torque(N.m)	14.3
Rated Power(kW)	3

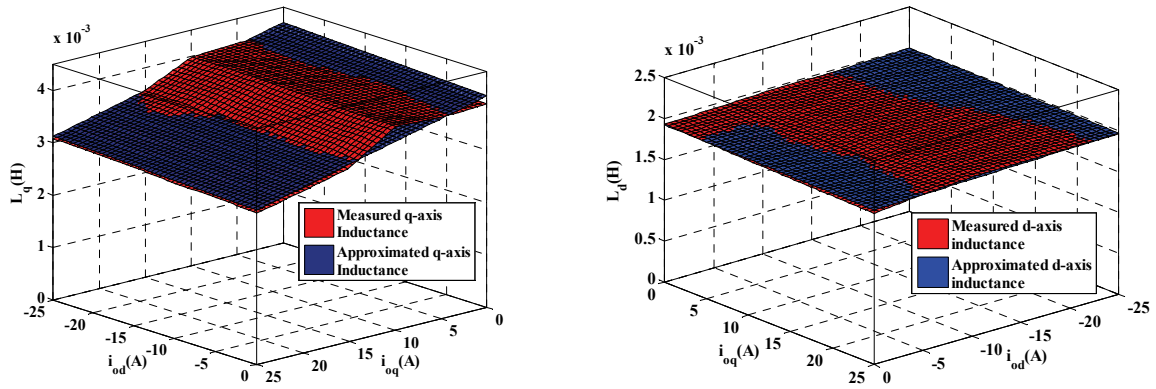

(a) (b)

Fig. 3. Motor parameters: (a) Measured and approximated L_q versus i_{od} and i_{oq}; (b) Measured and approximated L_d versus i_{oq} and i_{od}.

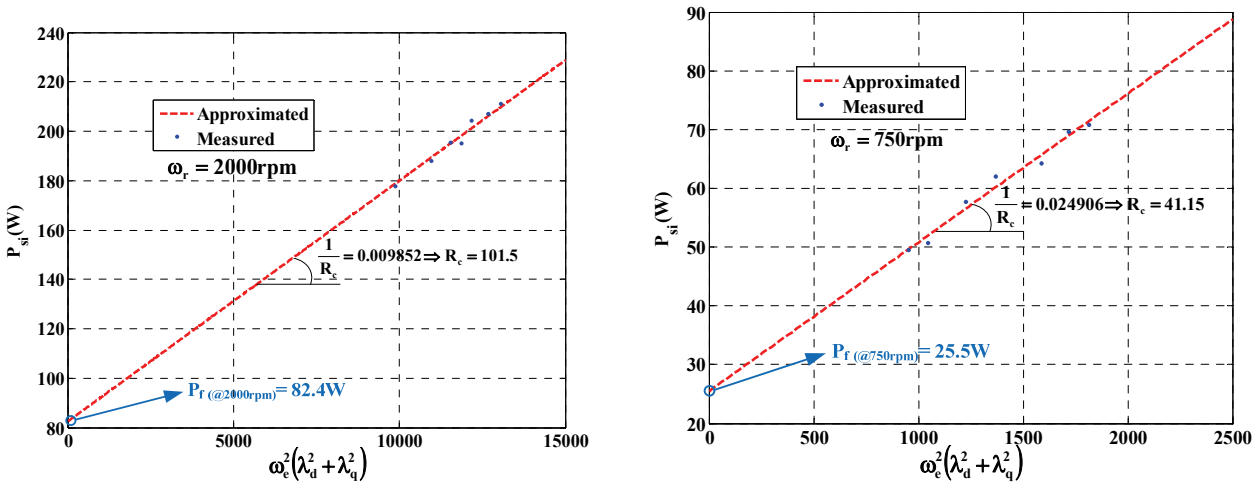

(a) (b)

Fig. 4. Semi-input power vs. the square of the speed emf at different speeds for obtaining the iron-loss resistance and sum of the mechanical and stray losses: (a) At 2000rpm; (b) At 750rpm.

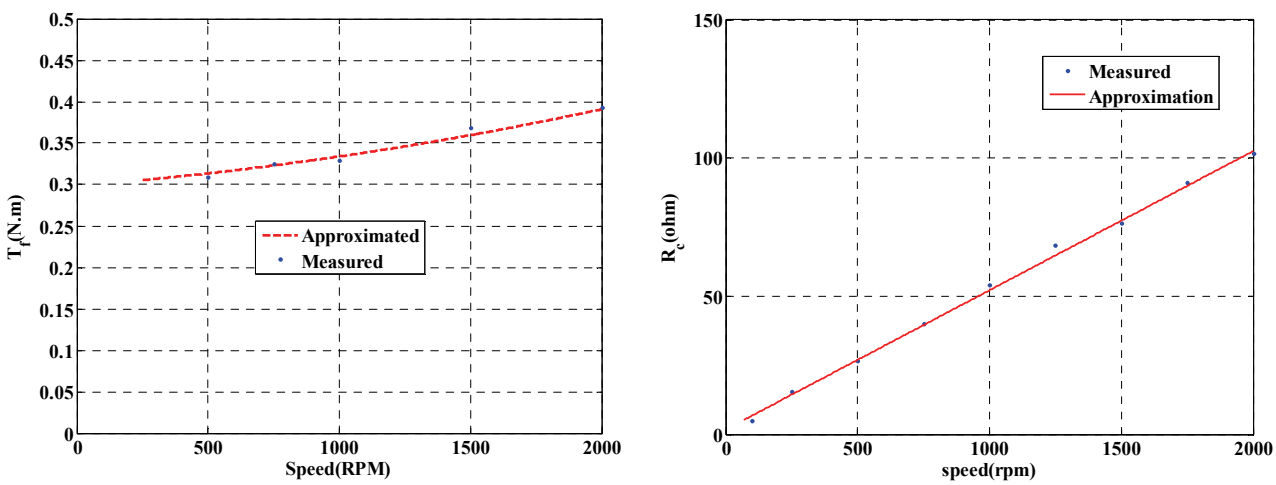

(a) (b)

Fig. 5. Iron loss resistance, mechanical loss and stray loss measurements (experimental results): (a) Measured sum of the mechanical and stray components of the torque (T_f) at different speeds; (b) Measured iron loss resistance vs speed.

speed. Typically, the semi-input power versus the square of the speed emf for 2000rpm and 750rpm are shown in Fig. 4(a) and Fig. 4(b). T_f for different speeds is illustrated in Fig. 5(a). In addition, the iron loss resistance is shown in Fig. 5(b).

TABLE II
TOTAL MOTOR LOSS AT 200RPM FOR THE LOSS MINIMIZATION CONTROL METHOD "WITH CONSIDERING SELF-SATURATION AND CROSS-SATURATION" AND "WITHOUT CONSIDERING SELF-SATURATION AND CROSS- SATURATION."

Load Torque	Method	Total Controllable Loss
4N.m	with considering self- and cross-saturation	20.9 W
	without considering self- and cross-saturation	20.9 W
8N.m	with considering self- and cross-saturation	45.4 W
	without considering self- and cross-saturation	46.1 W
12N.m	with considering self- and cross-saturation	83.6 W
	without considering self- and cross-saturation	85.0 W
14.3N.m	with considering self- and cross-saturation	112.1 W
	without considering self- and cross-saturation	114.6 W

VI. COMPARISON OF LOSS MINIMIZATION CONTROL METHODS (CONSIDERING THE SELF-SATURATION AND CROSS-SATURATION) WITH THE MTPA, UPF AND I_D=0 CONTROL METHODS

This section compares loss minimization control methods (considering self-saturation and cross-saturation) with the 'maximum torque per ampere,' 'unity power factor' and i_d=0 control methods for a fan type load. Fig. 6 shows the efficiency, copper loss, iron loss, volt-ampere, power factor and efficiency improvement of the loss minimization control methods in a comparison of the 'maximum torque per ampere,' 'unity power factor' and i_d=0 control methods at different speeds for a fan type load (where its load increases with speed).

The results of Fig. 7 are for the nominal speed (2000rpm) and at different load torques. As illustrated in Fig. 6(f) and Fig. 7(f), a significant efficiency improvement is obtained for the loss minimization control method in comparison with the other methods.

The efficiency improvement for the loss minimization control method in a comparison with the 'maximum torque per ampere' method decreases with an increment of the load. This is due to the fact that the 'maximum torque per ampere' method minimizes the copper loss without considering the iron loss. In addition, the optimum power factor approaches unity (based on results of the loss minimization control method) under heavy loads and high speeds. Therefore, the efficiency of the loss minimization control method and the 'unity power factor' method are close to each other under heavy loads and high speeds.

In order to compare the results of "with considering self-saturation and cross-saturation" and "without considering self-saturation and cross-saturation," the total controllable losses of these methods are compared in Table. II. The results of both methods in this table are in 200RPM.

As shown in results of Table II, as expected under light loads, considering self-saturation and cross-saturation does not have a significant impact on the motor loss. This is due to the fact that under light loads there is not considerable saturation. In addition, by increment of the load torque, the consideration of self-saturation and cross-saturation has a greater impact on the decrement of motor loss.

VII. EXPERIMENTAL RESULTS

To validate the applicability of the proposed method, a prototype has been constructed and shown in Fig. 8. The IPMSM parameters are listed in Table I. The IPMSM is controlled by a dsPIC microcontroller (dsPIC30f4011). An Advantech USB-4711A data acquisition apparatus is utilized for sampling results. A dc generator is coupled to the IPMSM as a load as shown in Fig. 8. The configuration of the test setup is illustrated in Fig. 9.

In the control system, a PI controller is used in the outer loop. The three outputs from the encoder, including the QEA, QEB and Index, are connected to pins related to the dsPIC Quadrature Encoder Interface (QEI) module to calculate the motor speed. The speed is calculated in a specified interval. This interval is determined based on the maximum specified speed. In addition, two PI-controllers are utilized in the inner loop for controlling the d-axis and q-axis currents. The outputs of these two controllers are V_d and V_q. Then, $V_{a,b,c}$ is obtained by implementing a Park transformation to V_d and V_q. Afterwards $V_{a,b,c}$ is set as the input of the dsPIC Motor Control PWM module.

At first, results for investigating the performance of the loss minimization control method (while considering self-saturation and cross-saturation) under speed command variations are shown in Fig. 10. In this test, the motor operates under the no-load condition. In addition, the speed command is 2000 rpm, which decreases to 200rpm at t=1sec. The d-axis current, q-axis current and speed are illustrated in Fig. 10.

In the second test, the performance of the loss minimization control method (while considering self-saturation and cross-saturation) is investigated under load variations and the results are shown in Fig. 11. In this test, the speed command is set to 2000rpm, the motor runs under the no-load condition (apart from the no-load loss of the dc-generator and the

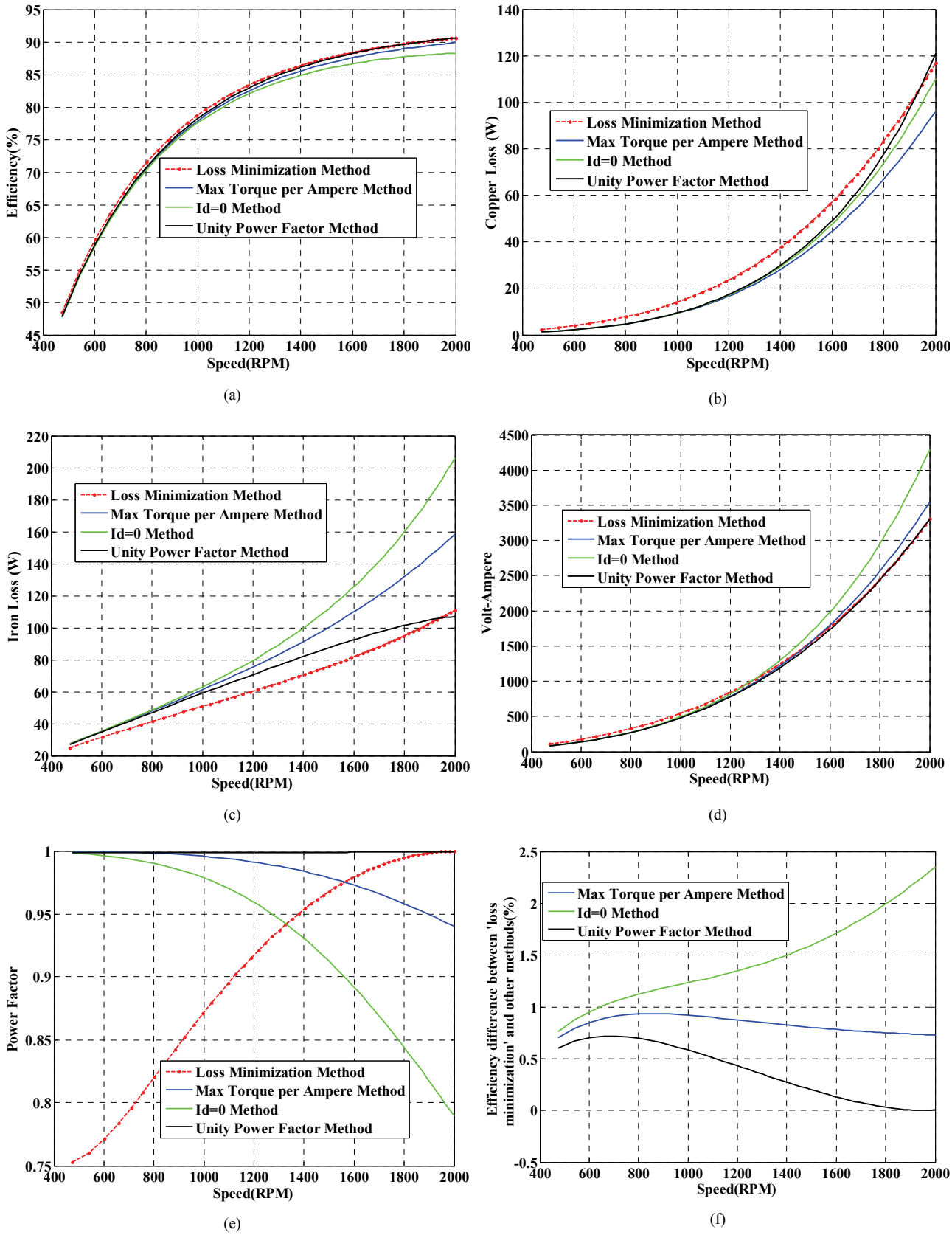

Fig. 6. Comparison of the loss minimization control method with the MTPA, UPF and i_d=0 control methods: (a) Efficiency vs. speed; (b) Copper loss vs. speed; (c) Iron loss vs. speed; (d) Volt-ampere vs. speed; (e) Power factor vs. speed; (f) Efficiency improvement of the loss minimization control method in comparison with the MTPA, UPF and i_d=0 control methods.

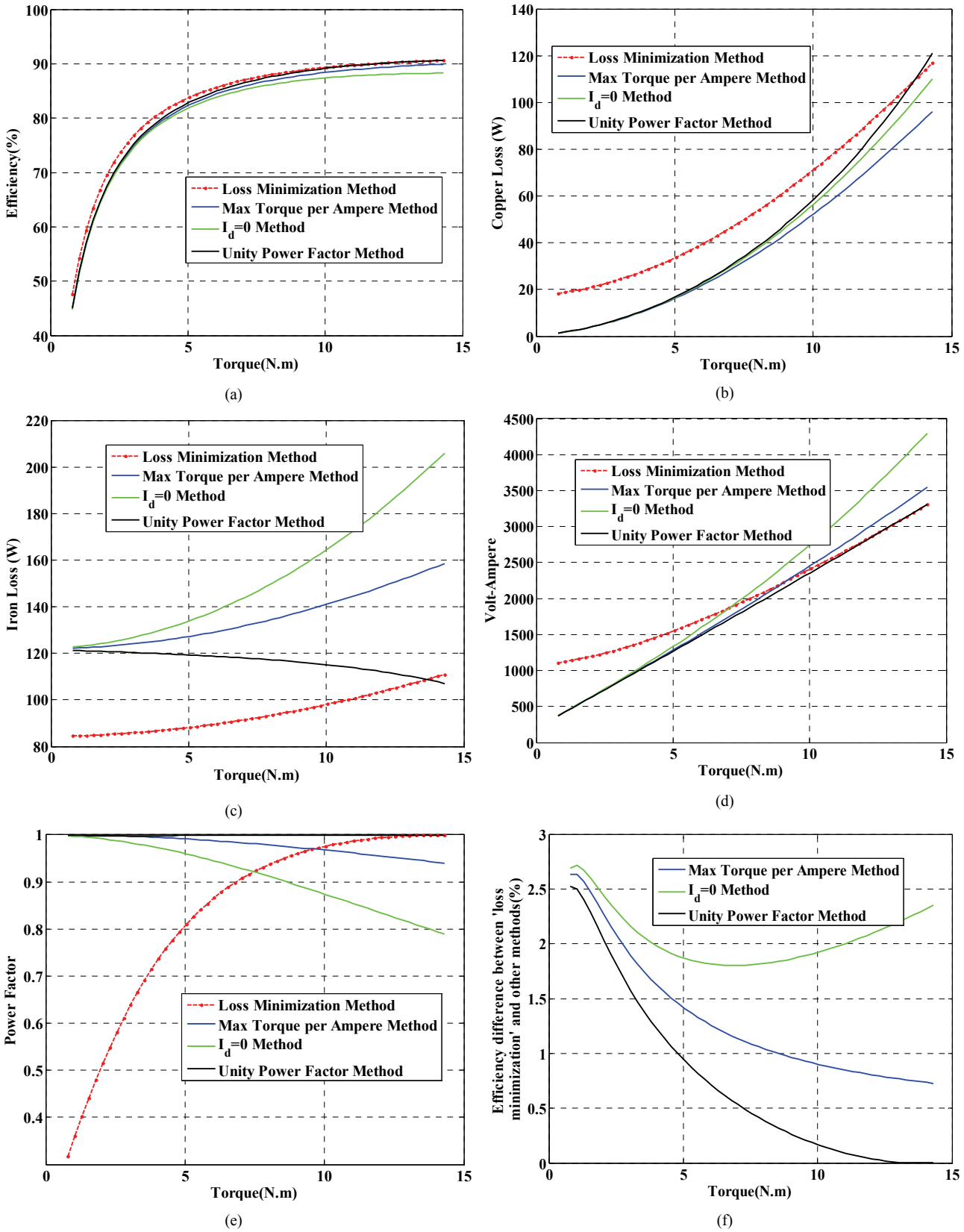

Fig. 7. Comparison of the loss minimization control method with the MTPA, UPF and i_d=0 control methods at a nominal speed (2000rpm) and under different load torques: (a) Efficiency vs. torque; (b) Copper loss vs. torque; (c) Iron loss vs. torque; (d) Volt-ampere vs. torque; (e) Power factor vs. torque; (f) Efficiency improvement of the loss minimization control method in comparison with the MTPA, UPF and i_d=0 control methods.

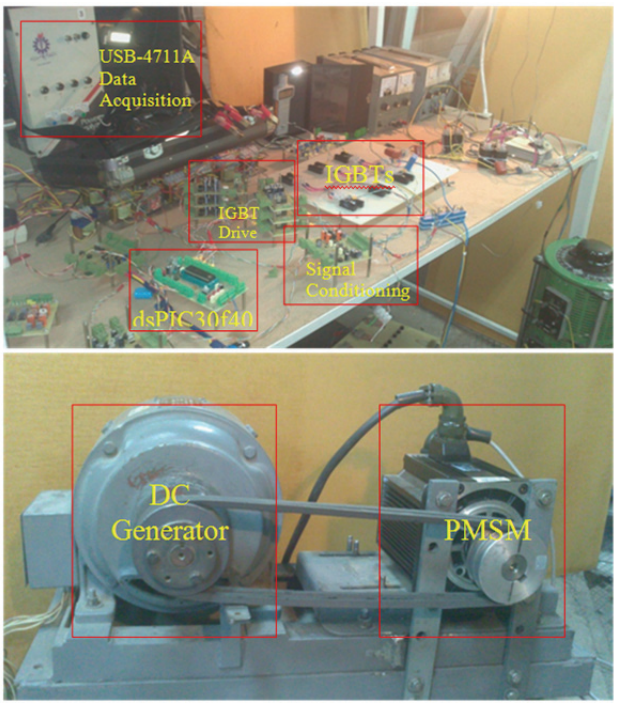

Fig. 8. Experimental setup.

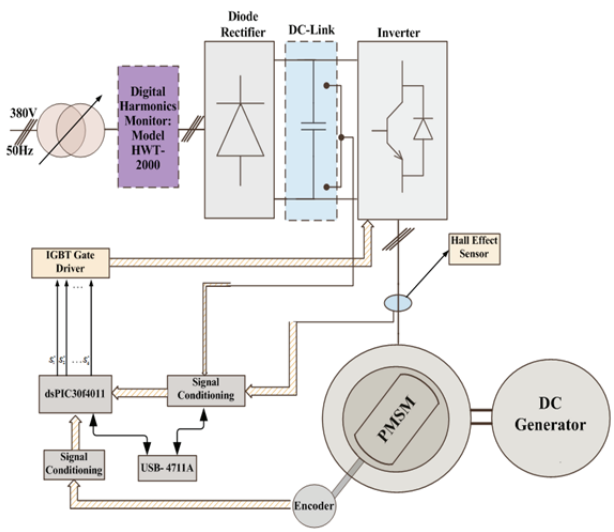

Fig. 9. Test setup configuration.

TABLE III
TOTAL CONTROLLABLE LOSS FOR THE LOSS MINIMIZATION CONTROL METHOD OBTAINED FROM THE CALCULATION AND EXPERIMENTAL RESULTS AT THE NOMINAL SPEED (2000RPM)

3N.m	Simulation	110.2 W
	Experimental	117.8 W
6N.m	Simulation	129.1 W
	Experimental	136.6 W
9N.m	Simulation	157.2 W
	Experimental	165.8 W
12N.m	Simulation	193.9 W
	Experimental	199.7 W

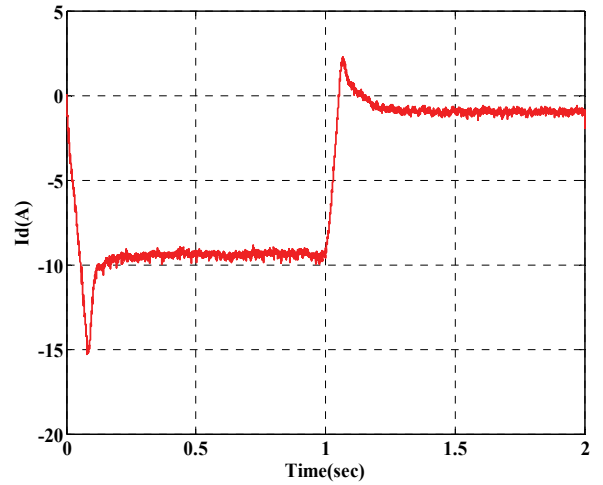

(a)

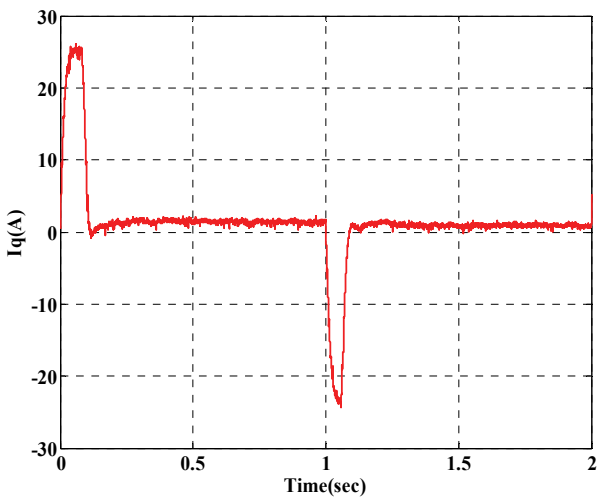

(b)

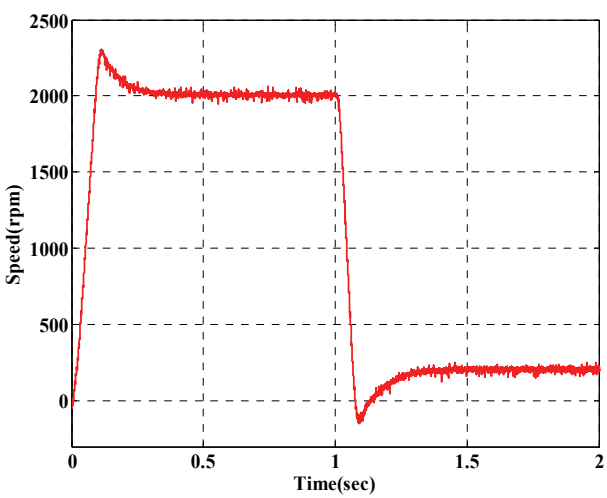

(c)

Fig. 10. Performance of the proposed method under variations of the speed reference without coupling to a dc generator (experimental result): (a) D-axis current; (b) Q-axis current; (c) Speed.

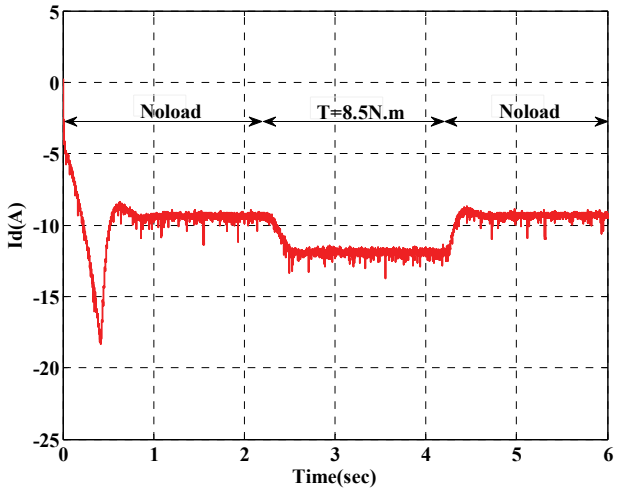

(a)

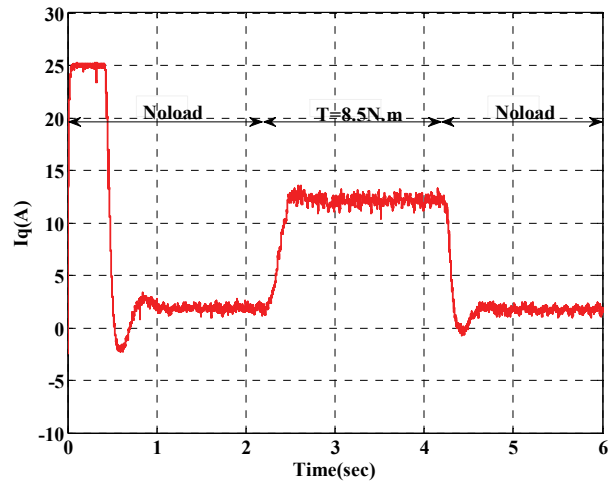

(b)

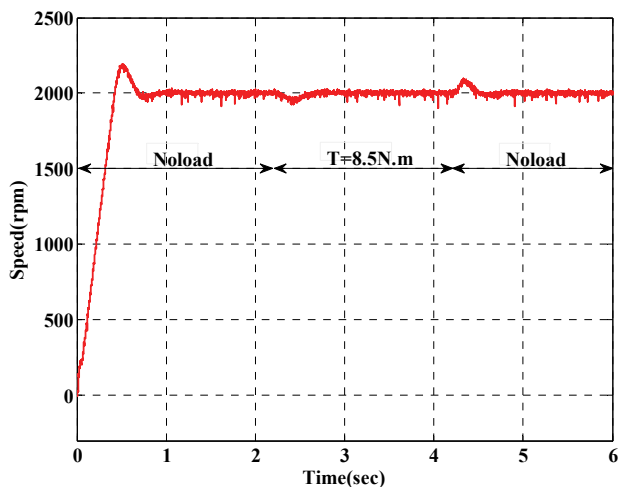

(c)

Fig. 11. Performance of the proposed method under step variations of the load torque (8.5N.m) with coupling to a dc generator (experimental result): (a) D-axis current; (b) Q-axis current; (c) Speed.

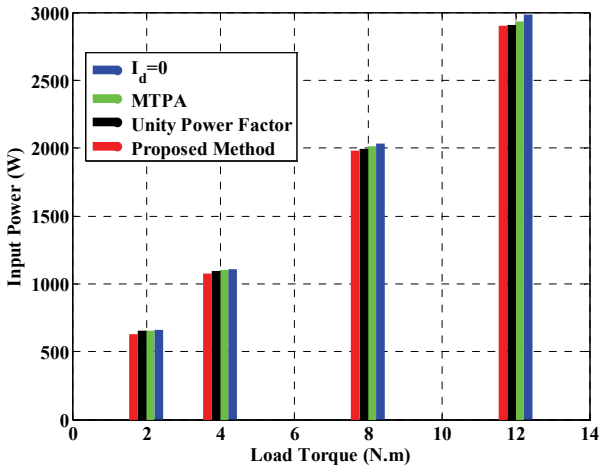

Fig. 12. Input power of the diode rectifier measured by a Digital Harmonic Monitor under different load torques at 2000RPM (experimental result).

coupling loss) and 8.5N.m is applied to the motor as a load at about t=2.2sec. Fig. 11 shows the d-axis current, q-axis current and speed.

For independent proof of the efficiency optimization, the input power of the diode-rectifier is measured for the different control methods. Experimental results for the proposed, MTPA, unity power factor and i_d=0 control methods are illustrated in Fig. 12. The input power of the diode rectifier under different load torques (2N.m, 4N.m, 8N.m and 12N.m) is shown in this figure. These load torques are achieved by adjusting the excitation and the variable resistive load of the dc generator (some variable resistive loads are placed in the output of the dc generator for adjusting the load torque by changing the value of these resistive loads). The experimental results of Fig. 12 are measured at the nominal speed (2000 rpm). These results show that the input power in the proposed method is lower than the input power in the other methods for different load torques.

In addition, simulation results are compared with experimental results under different load torques. Table III shows the total controllable loss including the copper loss and iron loss obtained from the simulation and experiments. They are shown to have good agreement with each other. In the experimental results, the sum of the output power and mechanical loss, obtained from Fig. 5(a), are subtracted from the input power in order to obtain the total controllable loss.

VIII. Conclusion

In this paper, a loss minimization control method considering self-saturation and cross-saturation is presented. Ignoring the self-saturation and cross-saturation in the loss minimization control method leads to an error in the optimum operating point. Therefore, by utilizing a linear approximation,

the effect of self-saturation and cross-saturation is considered in the loss minimization control method. In addition, the iron loss resistance variation due to frequency is considered in the proposed method.

A comparison of the loss minimization control method (considering self-saturation and cross-saturation) with the MTPA, UPF and i_d=0 control methods shows that a considerable efficiency improvement can be achieved. Furthermore, experimental results verified the applicability and proper dynamic response of the loss minimization control method considering self-saturation and cross-saturation.

REFERENCES

[1] R. Nalepa and T. Kowalska, "Optimum trajectory control of the current vector of a nonsalient-pole PMSM in the field-weakening region," *IEEE Trans. Ind. Electron*., Vol. 59, No. 7, pp. 2867-2876, Jul. 2012.

[2] S. Sul, *Control of Electric Machine Drive Systems*, IEEE Press series on power engineering, 2011.

[3] Y. Zhang, L. Xu, M. Güven, S. Chi, and M. Illindala, "Experimental verification of deep field weakening operation of a 50-kw IPM machine by using single current regulator," *IEEE Trans. Ind. Appl*., Vol. 47, No. 1, pp. 128-133, Jan./Feb. 2011.

[4] R. Krishnan, *Permanent Magnet Synchronous and Brushless DC Motor Drives*, Taylor & Francis Group, 2010.

[5] D. Stojan, D. Drevensek, Z. Planti, B. Grcar, and G. Stumberger, "Novel field-weakening control scheme for permanent-magnet synchronous machines based on voltage angle control," *IEEE Trans. Ind. Appl*,, Vol. 48, No. 6, pp. 2390-2401, Nov./Dec. 2012.

[6] Y. Xu, N. Parspour, and U. Vollmer, "Torque ripple minimization using online estimation of the stator resistances with consideration of magnetic saturation," *IEEE Trans. Ind. Electron*., Vol. 61, No. 9, pp. 5105-5114, Sep. 2014.

[7] S. Morimoto, Y. Takeda, T. Hirasa, and K. Taniguchi, "Expansion of operating limits for permanent magnet motor by current vector control considering inverter capacity," *IEEE Trans. Ind. Appl*., Vol. 26, No.5, pp. 866-871, Sep./Oct. 1990.

[8] Y. Nakamura, T. Kudo, F. Ishibashi, and S. Hibino, "High-efficiency drive due to power factor control of a permanent magnet synchronous motor," *IEEE Trans. Power Electron*., Vol. 10, No.2, pp. 247-253, Mar. 1995.

[9] E. Al-nabi, B. Wu, N. Zargari, and V. Sood, "Input power factor compensation for high-power CSC fed PMSM drive using d-axis stator current control," *IEEE Trans. Ind. Electron*., Vol. 59, No. 2, pp. 752-761, Feb. 2012.

[10] S. Bolognani, R. Petrella, A. Prearo, and L. Sgarbossa, "Automatic tracking of MTPA trajectory in IPM motor drives based on AC current injection," *IEEE Trans. Ind. Appl*., Vol. 47, No. 1, pp. 105-114, Jan./Feb. 2011.

[11] S. Kim, Y.D. Yoon, S.K. Sul, and K. Ide, "Maximum torque per ampere (MTPA) control of an IPM machine based on signal injection considering inductance saturation," *IEEE Trans. Power Electron*., Vol. 28, No. 1, pp. 488-497, Jan. 2013.

[12] A. Consoli, G. Scarcella, G. Scelba, and A. Testa "Steady-state and transient operation of IPMSMs under maximum-torque-per-ampere control," *IEEE Trans. Ind. Appl*., Vol. 46, No. 1, pp. 121-129, Jan./Feb. 2010.

[13] D. S. Kirschen, D. W. Novotny, and T. A. Lipo, "On-line efficiency optimization of a variable frequency induction motor drive," *IEEE Trans. Ind. Appl*., Vol. IA-21, pp. 610-616, May/Jun. 1985.

[14] F. Abrahamsen, F. Blaabjerg, J. K. Pedersen, and P. B. Thoegersen, "Efficiency-optimized control of medium-size induction motor drives," *IEEE Trans. Ind. Electron*., Vol. 37, No. 6, pp. 1761-1767, Nov./Dec. 2001.

[15] F. Abrahamsen, F. Blaabjerg, J. K. Pedersen, and P. B. Thoegersen, "On the energy optimized control of standard and high-efficiency induction motors in CT and HVAC applications," *IEEE Trans. Ind. Appl*., Vol. 34, No. 4, pp. 822-831, Jul./Aug. 1998.

[16] C. Chakraborty and Y. Hori, "Fast efficiency optimization techniques for the indirect vector-controlled induction motor drives," *IEEE Trans. Ind. Appl*., Vol. 39, No. 4, pp. 1070-1076, Jul./Aug. 2003.

[17] R. S. Colby, and D. W. Novotny, "An efficiency- optimizing permanent-magnet synchronous motor drive," *IEEE Trans. Ind. Appl*., Vol. 24, No. 3, pp. 462-469, May/Jun. 1988.

[18] C. Cavallaro, A. O. Tommaso, R. Miceli, A. Raciti, G. R. Galluzzo, and M. Trapanese, "Efficiency enhancement of permanent-magnet synchronous motor drives by online loss minimization approaches," *IEEE Trans. Ind. Electron*., Vol. 52, No. 4, pp. 1153-1160, Aug. 2005.

[19] S. Vaez, V. I. John, and M. A. Rahman, "An on-line loss minimization controller for interior permanent magnet motor drives," *IEEE Trans. Energy Convers*., Vol. 14, No. 4, pp. 1435-1440, Dec. 1999.

[20] S. Morimoto, Y. Tong, Y. Takeda, and T. Hirasa, "Loss minimization control of permanent magnet synchronous motor drives," *IEEE Trans. Ind. Electron*., Vol. 41, No. 5, pp. 511-517, Oct. 1994.

[21] C. Mademlis, I. Kioskeridis, and N. Margaris, "Optimal efficiency control strategy for interior permanent-magnet synchronous motor drives," *IEEE Trans. Energy Convers*., Vol. 19, No. 4, pp. 715-723, Dec. 2004.

[22] N. Urasaki, T. Senjyu, and K. Uezato, "A novel calculation method for iron-loss resistance suitable in modeling permanent-magnet synchronous motors," *IEEE Trans. Energy Convers*., Vol. 18, No. 1, pp. 41-47, Mar. 2003.

Hamidreza Pairo was born in Tehran, Iran, in 1986. He received his B.S., M.S. and Ph.D. degrees in Electrical Engineering from the Iran University of Science and Technology (IUST), Tehran, Iran, in 2008, 2011 and 2017, respectively. He is employed at the Iranian Research Institute of Electrical Engineering; Academic Center for Education, Culture and Research (ACECR), where he is presently working on the design and construction of medium voltage high power drives. His current research interests include high power drives, multilevel converters, multiphase motor drives, efficiency improvement of motor drives, power electronics and electrical machines.

Mohammad Khanzade was born in Ardakan, Iran, in 1962. He received his B.S. and M.S. degrees in Electrical Engineering from the Iran University of Science and Technology (IUST), Tehran, Iran, in 1988 and 1993, respectively. He received his Ph.D. degree from Semnan University, Semnan, Iran, in 2010. He is presently working as an Assistant Professor with the ICT Faculty of Imam Hosein Comprehensive University, Tehran, Iran. His current research interests include electric machinery, power electronics and pulsed power.

Abbas Shoulaie was born in Isfahan, Iran, in 1949. He received his B.S. degree from the Iran University of Science and Technology (IUST), Tehran, Iran, in 1973; and his M.S. and Ph.D. degrees in Electrical Engineering from Université des Sciences et Techniques du Languedoc (USTL), Montpellier, France, in 1981 and 1984, respectively. He is presently working as a Professor of Electrical Engineering at IUST. His current research interests include power electronics, magnetic systems, linear motors, flexible ac current transmission systems (FACTS), and high voltage dc (HVDC) systems.